Quantum Support Vector Regressor for Robust Channel Estimation in OFDM Systems

Daniel C. Neves, Felipe A. Silva, Demerson N. Gonçalves and João T. Dias

Abstract—**Channel estimation in OFDM systems is generally performed based on pilot symbols using least squares (LS). However, in a practical environment where impulse noise may be present, this method may not be effective. In this work we propose the use of quantum kernel in support vector machine (SVM) algorithm for robust channel estimation in OFDM systems and compare its performance with the LS and the classic support vector regressor (SVR). The viability of our approach is substantiated by computational simulation results obtained in frequency selective channel models with the presence of non-Gaussian impulsive noise interfering in the pilot symbols.**

Keywords—**Channel estimation, OFDM, SVR, QSVR.**

I. INTRODUCTION

Orthogonal Frequency Division Multiplexing (OFDM) has become a popular scheme for wireless networking standards that operate at a high bit rate [1]. The main advantage of OFDM over single-carrier schemes is its ability to eliminate intersymbol interference (ISI) without the need for complex equalization filters at the receiver [1]. Channel estimation in OFDM systems is usually performed based on pilot symbols using least squares (LS) [2]. However, in a practical environment where impulse noise may be present, this method may not be effective [3].

Support vector machines (SVM) have been proposed to solve a variety of problems in digital communications systems [4], including channel estimation [5]. However, when we observe non-linearities in the system, it is necessary to choose a kernel based on Mercer's conditions [6] and adjust its parameters to obtain an optimal regressor.

Quantum algorithms have been proposed to solve problems with prohibitive complexity in classical algorithms [7], including in communications systems [8], [9], [10]. In this work, we propose the use of a quantum kernel for the SVM regressor to channel estimation in an OFDM system with frequency selective channel and impulsive noise presence.

This article is divided as follows: in section II, the OFDM system and the noise model are described. The LS and SVR estimator models are presented in section III. In section IV, the quantum support vector regressor are presented. The results are shown in section V, and conclusions are made in section VI.

Daniel C. Neves, Coord. de Licenciatura em Física, CEFET-RJ, Petrópolis-RJ, e-mail:daniel.neves@aluno.cefet-rj.br; Felipe A. Silva, Coord. de Licenciatura em Matemática, CEFET-RJ, Petrópolis-RJ, e-mail: felipe.silva.6@aluno.cefet-rj.br; Demerson N. Gonçalves, Coord. de Licenciatura em Matemática, CEFET-RJ, Petrópolis-RJ, e-mail:demerson.goncalves@cefet-rj.br; João T. Dias, Dep. de Engenharia de Telecomunicações, CEFET-RJ, Rio de Janeiro-RJ, e-mail: joao.dias@cefet-rj.br. This work was partially supported by Cefet/RJ, Faperj and CNPq.

II. SIGNAL MODEL

The block diagram of the implemented OFDM system is shown in Fig. 1. In this system, b are the bits to be transmitted, s are the frequency domain data symbols, x are the time domain data samples, y is the received signal in the time domain, $\hat{s}$ is the received signal in the frequency domain and $\hat{b}$ are the estimated bits.
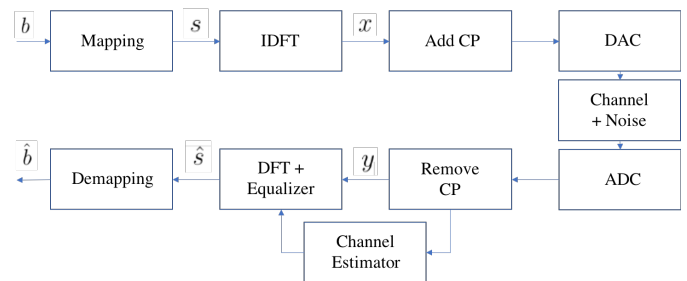

Fig. 1. Block diagram of the implemented OFDM system.

The OFDM signal can be expressed in the time domain by [1]

$$x[n] = \sum_{k=0}^{K-1} s_k e^{j2\pi \frac{k}{K}n}, \qquad (1)$$

where $\mathbf{s}_k$ is the data symbol on the k-th subcarrier and K is the number of subcarriers in the OFDM symbol.

The signal at the receiver can be written by

$$y[n] = \sum_{k=0}^{K-1} s_k H_k e^{j2\pi \frac{k}{K}n} + \omega_n + b_n g_n, \qquad (2)$$

where $y[n]$ are time-domain sample before DFT transformation, H_k is the channel's frequency response at the kth frequency, ω_n is additive white Gaussian noise (AWGN), and $b_n g_n$ is the impulse noise modeled as a Bernoulli–Gaussian process, i.e., the product of a real Bernoulli process b_n with $Pr(b_n = 1) = p$ and a complex Gaussian process g_n [11].

Then, residual noise at the receiver side is given by the sum of both terms $z_n = \omega_n + b_n g_n$.

III. CHANNEL ESTIMATORS

The channel estimation can be done in the time domain or in the frequency domain. In OFDM systems, pilot symbols S_p are usually inserted between data symbols for channel estimation purposes. Then, the channel's frequency response can be first estimated over a subset of subcarriers (pilot positions), with cardinality κ_p, and then interpolated over the remaining subcarriers. It is well known that if the channel

impulse response has a maximum of L resolvable paths (and hence of degrees of freedom), then κ_p must be at least equal to L [12].

The estimators that will be used in the performance comparison in this work are:

A. LS

The least squares (LS) channel estimator obtains the estimate of the frequency response of the channel at the position of the pilot tones as [13]

$$\hat{H}(k) = \frac{\hat{s}_p(k)}{s_p(k)}, \qquad (3)$$

where $\hat{s}_p(k)$ is the received signal on the kth subcarrier in frequency domain and $s_p(k)$ is the pilot signal transmitted on the kth subcarrier. After the estimation, a linear interpolation is used to obtain the channel frequency response in all subcarrier of the OFDM symbol.

B. SVR

The Support Vector Regressor (SVR) uses $\{(\mathbf{x}_1, y_1), ..., (\mathbf{x}_l, y_l)\} \subset \mathcal{X} \times \mathbb{R}$, where $\mathcal{X}$ is the input space, as a training dataset, to find the function

$$f(\mathbf{x}) = \langle \omega, \mathbf{x} \rangle + b, \qquad (4)$$

that has at most ε deviation from the actually targets y_i, and at the same time is as flat as possible [14].

The OFDM system with the pilot tones can be viewed in the time domain as

$$y[n] = \sum_{k \in \kappa_p} s_p(k) H_p(k) e^{j2\pi \frac{k}{K} n} + \sum_{k \notin \kappa_p} s(k) H(k) e^{j2\pi \frac{k}{K} n} + z_n, \qquad (5)$$

and the signal model for OFDM-SVR is as follows:

$$y[n] = \sum_{k \in \kappa_p} s_p(k) H_p(k) e^{j2\pi \frac{k}{K} n} + e_n, \qquad (6)$$

where $e_n = \sum_{k \notin \kappa_p} s(k) H(k) e^{j2\pi \frac{k}{K} n} + z_n$ contains the residual noise plus the term due to data symbols. Here, these unknown symbols carrying information will be considered as noise during the training phases.

As the SVR was proposed to act on samples of real values [14] and OFDM symbols have complex values, the proposed SVR estimator will be divided into two estimators acting in parallel, one on the real part of the OFDM symbol $\Re(y[n])$ and the other on the imaginary part $\Im(y[n])$.

Considering the slack variables ξ_i and ξ_i^*, respectively, for the positive and negative components in the real part, we arrive at a formulation whose task boils down to minimizing

$$\frac{1}{2} \|H_p(k)\|^2 + C \sum_{i=1}^{l} (\xi_i + \xi_i^*), \qquad (7)$$

subject to

$$\Re(y[n]) - \sum_{k \in \kappa_p} \Re(s_p(k) H_p(k) e^{j2\pi \frac{k}{K} n}) \le \varepsilon + \xi_i; \qquad (8)$$

$$-\Re(y[n]) + \sum_{k \in \kappa_p} \Re(s_p(k) H_p(k) e^{j2\pi \frac{k}{K} n}) \le \varepsilon + \xi_i^*; \qquad (9)$$

$$\xi_i, \xi_i^* \le 0. \qquad (10)$$

In the imaginary part, a similar procedure is performed. The positive constant C determines the trade-off between the flatness of f and the amount up to which deviations larger than ε are tolerated [14].

By making zero the primal-dual functional gradient with respect to $H_p(k)$, we get the Lagrange multipliers φ_n and φ_n^* for the positive and negative components, respectively. The expression for channel estimated real values at pilot positions is:

$$\Re(\hat{H}_p(k)) = \sum_{n=1}^{K-1} (\varphi_n - \varphi_n^*) \Re(s_p(k)). \qquad (11)$$

After estimating the real and imaginary parts of $\hat{H}_p(k)$, we join the values to obtain the complex estimation of $\hat{H}_p(k)$.

Until here, the equations were formulated for a linear scenario. The interesting in this method is that exist a strategy that transforms a non-linear problem into a linear problem [14]. This strategy is called "kernel trick".

Give a map function $\phi : \mathcal{X} \to \mathcal{F}$, is possible rewrite non-linear regression problem as a linear regression problem in feature space $\mathcal{F}$.

The kernel is defined as

$$k(x, x') = \langle \phi(x), \phi(x') \rangle. \qquad (12)$$

IV. QUANTUM SUPPORT VECTOR REGRESSOR

A. Basics of quantum computing

Quantum computing is a model of computation that exploits quantum mechanical phenomena by harnesses the power of atomic and subatomic particles to perform high speed parallel computing [15]. Classical information in digital computers is represented by logical binary digits (bits). A logical bit can take the value of 1 or 0 depending on whether the voltage in the wire is High or Low in a logic circuit. In contrast, the smallest unit of information stored in a two-state quantum computer, called a *quantum bit* or *qubit*, is a unit vector in the two-dimensional complex Hilbert space ($\mathbb{C}^2$) for which a particular orthogonal basis $\{|0\rangle, |1\rangle\}$ has been fixed.

The quantum state of a qubit can be represented using any chosen orthogonal basis. The most commonly used basis is the *computational basis*, which corresponds to $|0\rangle = [1, 0]^T$ and $|1\rangle = [0, 1]^T$. Unlike the classical bit, a qubit can be in a linear superposition of $|0\rangle$ and $|1\rangle$,

$$|\psi\rangle = \alpha |0\rangle + \beta |1\rangle = [\alpha, \beta]^T, \qquad (13)$$

where $\alpha, \beta \in \mathbb{C}$ are the *amplitudes* of $|\psi\rangle$ on the computational basis with the constraint $|\alpha|^2 + |\beta|^2 = 1$. When $\alpha = 1$, then $\beta = 0$ and hence $|\psi\rangle = |0\rangle$, which corresponds to the classical bit value 0. Similarly, if $\alpha = 0$, then $\beta = 1$ and $|\psi\rangle = |1\rangle$, which corresponds to the classical bit value 1. In general, when a state of one qubit $|\psi\rangle$ is *measured* with respect to the computational basis, the probability that the measured value is $|0\rangle$ is $|\alpha|^2$ and the probability that the measured value is $|1\rangle$ is $|\beta|^2$.

The state of a quantum computer can be changed by applying unitary operators or quantum gates to its qubits [15]. One of the most widely used single-qubit unitary operator is the Hadamard gate, given by

$$H = \frac{1}{\sqrt{2}} \begin{bmatrix} 1 & 1 \\ 1 & -1 \end{bmatrix}. \tag{14}$$

One can easily check that $H |0\rangle = \frac{|0\rangle + |1\rangle}{\sqrt{2}}$ and $H |1\rangle = \frac{|0\rangle - |1\rangle}{\sqrt{2}}$. If the input is $|0\rangle$, the Hadamard gate creates a superposition of states with equal weights.

Another important set of single-qubit gates is the *Pauli matrices*,

$$X = \begin{bmatrix} 0 & 1 \\ 1 & 0 \end{bmatrix}, Y = \begin{bmatrix} 0 & -i \\ i & 0 \end{bmatrix}, Z = \begin{bmatrix} 1 & 0 \\ 0 & -1 \end{bmatrix}. \tag{15}$$

The gate X is the quantum NOT gate because $X |\psi\rangle = \beta |0\rangle + \alpha |1\rangle$. The Z operator is the gate imposing a *phase shift* by π radians, since it flips the sign of the amplitude of the state $|1\rangle$, $Z |\psi\rangle = \alpha |0\rangle - \beta |1\rangle$. The operator Y can be considered as a combination of X and Z gates, because $Y |\psi\rangle = i(-\beta |0\rangle + \alpha |1\rangle)$.

In order to increase the complexity of a quantum system, a most general 1-qubit gate can be used:

$$U(\theta, \phi, \lambda) = \begin{bmatrix} \cos(\frac{\theta}{2}) & -e^{i\lambda} \sin(\frac{\theta}{2}) \\ e^{i\lambda} \sin(\frac{\theta}{2}) & e^{i(\lambda+\phi)} \cos(\frac{\theta}{2}) \end{bmatrix}. \tag{16}$$

For instances, three useful gates obtained from U are

$$U(\theta, \frac{\pi}{2}, -\frac{\pi}{2}) = R_x(\theta) = \begin{bmatrix} \cos(\frac{\theta}{2}) & -i \sin(\frac{\theta}{2}) \\ -i \sin(\frac{\theta}{2}) & \cos(\frac{\theta}{2}) \end{bmatrix}, \tag{17}$$

$$U(\theta, 0, 0) = R_y(\theta) = \begin{bmatrix} \cos(\frac{\theta}{2}) & -\sin(\frac{\theta}{2}) \\ \sin(\frac{\theta}{2}) & \cos(\frac{\theta}{2}) \end{bmatrix}, \tag{18}$$

$$U(0, 0, \lambda) = e^{\frac{i\lambda}{2}} R_z(\lambda) = \begin{bmatrix} 1 & 0 \\ 0 & e^{i\lambda} \end{bmatrix}, \tag{19}$$

where R_x, R_y and R_z are the operators that rotate the Bloch sphere about the x, y, and z-axis, respectively. Fig. 2 shows a Bloch sphere.
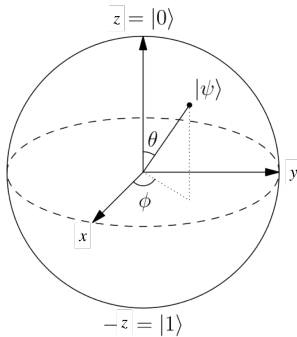

Fig. 2. Bloch sphere.

To dealing with multiple qubits is necessary to introduce the concept of *tensor product*. Let V and W be complex vectors space of dimensions m and n, respectively. The tensor product $V \otimes W$ is an mn-dimensional vector space.

For example, if we have a 2-qubit quantum computer and the first qubit is in the state $|0\rangle$ and the second is in the state $|1\rangle$, then the quantum computer is in the state $|0\rangle \otimes |1\rangle = |01\rangle = [0, 1, 0, 0]^T$. The resulting vector is a four-dimensional vector space. The general state $|\psi\rangle$ of a 2-qubit is a superposition $|\psi\rangle = \alpha |00\rangle + \beta |01\rangle + \gamma |10\rangle + \delta |11\rangle$, with the constraint $|\alpha|^2 + |\beta|^2 + |\gamma|^2 + |\delta|^2 = 1$.

In general, the quantum state $|\psi\rangle$ of an n-qubit is a superposition of 2^n states $|0\rangle, |1\rangle, \dots, |2^n - 1\rangle$ (computational basis in decimal notation),

$$|\psi\rangle = \sum_{i=0}^{2^n-1} \alpha_i |i\rangle, \tag{20}$$

with the amplitudes α_i constrained to $\sum_{i=0}^{2^n-1} |\alpha_i|^2 = 1$.

Applying the Hadamard gate to the n-qubit state $|0\rangle$ we obtain

$$H^{\otimes n} |0\rangle = \left(\frac{|0\rangle + |1\rangle}{\sqrt{2}} \right)^{\otimes n} = \frac{1}{\sqrt{2^n}} \sum_{i=0}^{2^n-1} |i\rangle. \tag{21}$$

The tensor product decribed in Eq. (21) produces an equally weighted superposition of all computational basis states, when the input is the state $|0\rangle$. This state is useful for applying *quantum parallelism*. Quantum parallelism is one of the most important features of quantum computers that promise to solve problems that are to hard for classical computers to solve in reasonable amount of time.

To conclude this discussion of basics of quantum computing, let us consider the most important operation on 2-qubit system, the *controlled-NOT* or *CNOT* gate. It has two input qubits, the *control* and the *target* qubit, respectively. The target qubit is flipped only if the control qubit is set to 1, that is, $|a, b\rangle \to |a, a \oplus b\rangle$, where $\oplus$ is addition modulo 2.
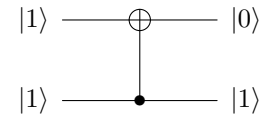

Fig. 3. CNOT gate with the second qubit as the control and the first qubit as the target.

B. Quantum kernels

For using the quantum computing and all their advantages is needed encoding the classical data $\mathbf{x}$ into a quantum state $|\psi\rangle$ [16]. In quantum computing universe, the quantum state $|\psi\rangle$, that describes completely the qubit, lives in Hilbert space $\mathcal{H}$ and this allows a very natural definition of a quantum kernel [16]. The classical data $\mathbf{x}$ is mapped in quantum state $|\psi\rangle$ through the map function $\phi : \mathcal{X} \to \mathcal{H}$. Then, the *quantum kernel* is defined as

$$k(\mathbf{x}, \mathbf{x}') = |\langle \phi(\mathbf{x}) | \phi(\mathbf{x}') \rangle|^2, \tag{22}$$

where $|\phi(\mathbf{x})\rangle = \mathcal{U}_{\phi(\mathbf{x})} |0\rangle$ and the circuit $\mathcal{U}_{\phi(\mathbf{x})}$ encodes the classical data $\mathbf{x}$ in quantum state $|\phi(\mathbf{x})\rangle$, for some unitary operator $\mathcal{U}$. The state $\langle \phi(\mathbf{x})|$ is the dual vector of $|\phi(\mathbf{x})\rangle$, obtained by transposing $|\phi(\mathbf{x})\rangle$ and conjugating each entry, in notation $\langle \phi(\mathbf{x})| = |\phi(\mathbf{x})\rangle^\dagger$.

The kernel defined in Eq. (22) can be efficiently estimated by a quantum computer using the well known SWAP Test [17]. The SWAP Test is a procedure commonly used in quantum machine learning to compare two quantum states by applying Hadamard gate in the first qubit and CNOT gates to each qubit, see Fig. 4.
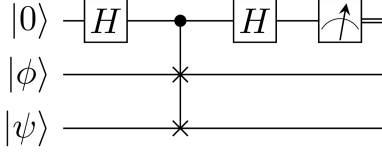

Fig. 4.   Circuit implementing the swap test between two states $|\phi\rangle$ and $|\psi\rangle$.

In this article we present a 5-qubit quantum support vector regressor (QSVR) for channel estimation in OFDM system. The main idea uses a quantum function to load classical data represented by pilot symbols into quantum states. The quantum feature map of depth d used in this work is defined by the unitary operator [18]

$$\mathcal{U}_{\Phi(\mathbf{x})} = \prod_d U_{\Phi(\mathbf{x})} H^{\otimes n}, \tag{23}$$

where

$$U_{\Phi(\mathbf{x})} = \exp\left(i \sum_{S\subseteq[n]} \phi_S(\mathbf{x}) \prod_{k\in S} Z_k\right). \tag{24}$$

The number n of qubits is equal to the dimensionality of the classical data $\mathbf{x}$, which in our case corresponds to the number of pilot tones used in OFDM system proposed. The symbols are encoded through the coefficients $\phi_S(\mathbf{x})$, where $S \subseteq [n] = \{1, \ldots, n\}$ describes all possible connections of qubits in the quantum circuit [18]. The encoding function is given by

$$\phi_S : x \mapsto \begin{cases} x_i & \text{if } S = \{i\} \\ (\pi - x_i)(\pi - x_j) & \text{if } S = \{i, j\} \end{cases} \tag{25}$$

and Z_k is the Z Pauli matrix acting on the k-th qubit.

For example, a quantum circuit that implements $\mathcal{U}_{\Phi(\mathbf{x})}$ using a single-qubit Z rotation, two-qubit ZZ rotation and interactions between all qubit pairs will produce blocks of the form
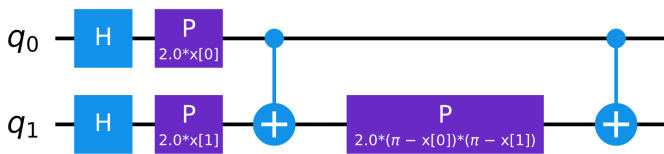

Fig. 5.   Quantum circuit of $\mathcal{U}_{\Phi(\mathbf{x})}$ with $n = 2$ qubits, depth $d = 1$ and Pauli rotation $P = R_Z$.

The Fig. 6 depicts a general circuit diagram for $\mathcal{U}_{\Phi(\mathbf{x})}$ with layers of Hadamard gates interleaved with entangling blocks encoding the classical data.

The difference between SVR and QSVR is the origin of the kernel. If kernel is calculated using quantum algorithms, that
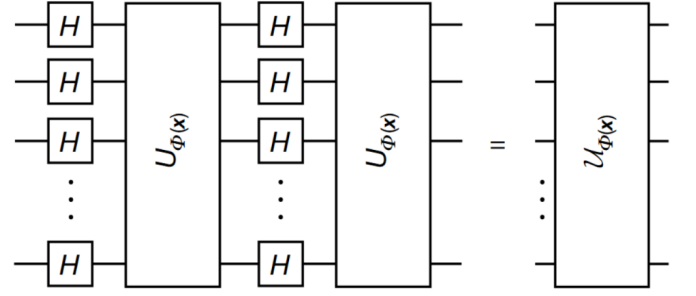

Fig. 6.   Quantum circuit of $\mathcal{U}_{\Phi(\mathbf{x})}$ with depth $d = 2$ and layers of Hadamard gates.

is, it's a quantum kernel then it's about QSVR. On the other hand, it's about SVR.

V. RESULTS

To validate the proposed quantum kernel for the SVR and compare its performance with the classic SVR and the LS in channel estimation in OFDM systems, bit error rate (BER) curves were created, considering the following simulation parameters:

TABLE I
SIMULATION PARAMETERS

number of subcarriers [K]	16
subcarrier modulation	16-QAM
cyclic prefix length in number of subcarriers	4
number of pilot subcarriers [S_p]	5

The tests were performed on a frequency selective channel with a delay profile given by $\mathbf{h} = [1\ 0\ 0.3+0.3j]$, and impulse noise distortion modeled with a Bernoulli–Gaussian process with $p = 0.05$. The impulse power in impulsive noise is fixed at 20 dB greater than the signal variance at the receiver input.

We consider a packet-based transmission, where each packet consists of a header at the beginning of the packet with a known training sequence or preamble to carry out channel estimation, followed by the OFDM data symbols. At the preamble, there are one OFDM symbol with pilot subcarriers. After the estimation (with either QSVR, SVR or LS) of channel coefficients at pilot positions $\hat{H}_p(k)$, we use them to compute the interpolation of the channel. Next, we perform zero forcing (ZF) equalization [19] using the interpolated channel. Detection is carried out with a hard-decision slicer over the equalized data. For each estimator, 100 packets were transmitted to calculate the average and raising the BER.

We studied the performance variation in the system due to changes in the kernel and free parameters of the SVR. We tested the linear, radial and polynomial kernels and varied the C parameter from 1 to 1000. The optimal parameter found for C was $C = 100$, and RBF kernel. Fig. 7 shows the BER performance as a function of the signal-to-noise ratio (E_b/N_0).

We also utilized the Qiskit library (an open-source quantum computing framework created by IBM®) [20] for the quantum machine learning task and a local quantum simulator. The
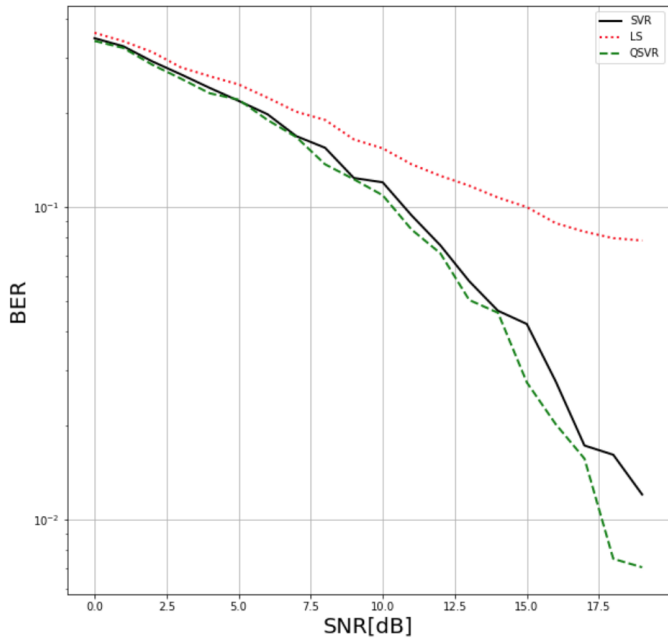
Fig. 7.   BER performance comparison.

classical kernel-based method for SVR was run on a classical computer with a regular CPU.

Analyzing the performance of the BER obtained from the three tested estimators, we can observe in the Fig. 7 that the BER curve obtained with the LS estimator decays very slowly up to 17.5 dB of SNR and presents a plateau from this value onwards, which shows its sensitivity to impulsive noise, while the curves obtained with the SVR and QSVR estimators show similar behavior and robustness to impulsive noise, with a slightly better performance for the QSVR, which can be explained by a better suitability of the quantum kernel for linearization of the input space data.

VI. CONCLUSIONS

In this work, an SVR algorithm with a quantum kernel for channel estimation in OFDM systems was proposed. Therefore, the structure of the adopted OFDM system, the channel estimation process in the time domain, by the SVR, and the frequency domain, by the LS, in addition to the fundamentals of quantum computing for generating the quantum kernel were described. Several tests were carried out in search of the optimal parameters of the SVR and the OFDM system. The simulations confirmed the robustness of the QSVR in the presence of impulse noise interfering with the pilot symbols and the results show that the proposal outperforms the classic SVR and the LS. Following this work, we intend to investigate the performance of QSVR in channel estimation and data detection in massive multiple-input, multiple-output OFDM systems (MIMO-OFDM), with multiple users and low resolution digital-to-analog converters (ADCs).

ACKNOWLEDGEMENTS

REFERENCES

[1] N. Marchetti, M. I. Rahman, S. Kumar, R. Prasad, *New Directions in Wireless Communications Research*, cap. 2, OFDM-Principles and Challenges, 2009.

[2] O. Edfors, M. Sandell, J. van de Beek, S.Wilson, and P. O. Börjesson, *Analysis of DFT-based channel estimators for OFDM* Div. Signal Process., Luleå Univ. Technol., Sweden, Res. Rep. TULEA, 1996, vol. 17.

[3] D. Shrestha, X. Mestre and M. Payaró, *On channel estimation for power line communication systems in the presence of impulsive noise*, Computers & Electrical Engineering, Volume 72, Pages 406-419, 2018.

[4] L. V. Nguyen, D. H. N. Nguyen, and A. L. Swindlehurst, *SVM-based channel estimation and data detection for massive MIMO systems with one-bit ADCs* to appear at IEEE Int. Conf. Commun., 2020.

[5] M. P. Sánchez-Fernández, M. de Prado-Cumplido, J. Arenas-García, and F. Pérez-Cruz, *SVM multiregression for nonlinear channel estimation in multiple-input multiple-output systems*, IEEE Trans. Signal Process., vol. 52, no. 8, pp. 2298–2307, Aug. 2004.

[6] D. Sebald and A. Buclew, *Support vector machine techniques for nonlinear equalization*, IEEE Trans. Signal Process., vol. 48, no. 11, pp.3217–3226, Nov. 2000.

[7] D. Neves, J. Drago, E. Dalcumune, D. Gonçalves, J. Dias, *Q-SVM Applied to Multi-User Detection in DS-CDMA Systems*. In: VI Workshop Escola de Computação e Informação Quântica, 2022, Alfenas. VI WECIQ, 2022.

[8] P. Botsinis, S. X. Ng and L. Hanzo. *Quantum Search Algorithms, Quantum Wireless, and a Low-Complexity Maximum Likelihood Iterative Quantum Multi-User Detector Design* in IEEE Access, vol. 1, pp. 94-122, 2013, doi: 10.1109/ACCESS.2013.2259536.

[9] P. Botsinis, D. Alanis, Z. Babar, S. X. Ng and L. Hanzo. *Joint Quantum-Assisted Channel Estimation and Data Detection* in IEEE Access, vol. 4, pp. 7658-7681, 2016, doi: 10.1109/ACCESS.2016.2591903.

[10] S. J. Nawaz, S. K. Sharma, S. Wyne, M. N. Patwary and M. Asaduz-zaman. *Quantum Machine Learning for 6G Communication Networks: State-of-the-Art and Vision for the Future* in IEEE Access, vol. 7, pp. 46317-46350, 2019, doi: 10.1109/ACCESS.2019.2909490.

[11] M. Ghosh, *Analysis of the effect of impulse noise on multicarrier and single carrier QAM systems*, IEEE Trans. Commun., vol. 44, no. 2, pp. 145–147, Feb. 1996.

[12] M. J. Fernández-Getino García, J. M. Páez-Borrallo, and S. Zazo, *DFT-based channel estimation in 2D-pilot-symbol-aided OFDM wireless systems*, in Proc IEEE Vehicular Technology Conf., 2001, vol. 2, pp. 815–819.

[13] A. Papoulis, *Probability Random Variables and Stochastic Processes*, McGraw-Hill, NY, 3 edition, 1991.

[14] Smola, A.J., Schölkopf, B. *A tutorial on support vector regression*. Statistics and Computing 14, 199–222 (2004).

[15] M. Nielsen, and I. Chuang. *Quantum Computation and Quantum Information*. Cambridge University Press, 2010.

[16] Schuld, M.; Petruccione, F. *Supervised learning with quantum computers*. Cham: Springer, 2018.

[17] H. Buhrman, R. Cleve, J. Watrous, and R. De Wolf. *Quantum finger-printing*. Phys. Rev. Lett. v. 87, 2001.

[18] Havlíček, V., Córcoles, A.D., Temme, K. et al. *Supervised learning with quantum-enhanced feature spaces*. Nature 567, 209–212 (2019).

[19] U. Katare, P. Patidar e A.C. Tiwari, *Comparative Analysis of ZF and MMSE Receiver for Multicode MC-CDMA Downlink Channels*. International Journal of Engineering Science and Innovative Technology (IJESIT) Volume 3, Issue 4, Julho 2014.

[20] Qiskit Community. *Qiskit Machine Learning overview*. https://qiskit.org. (Last accessed: 24.04.2023).